UHF-RFID-Based Localization Using Spread-Spectrum Signals

Andreas Loeffler
Chair of Information Technologies
Friedrich-Alexander-University of Erlangen-Nuremberg
Erlangen, Germany
Email: loeffler@like.eei.uni-erlangen.de

***Abstract*—Determining the range between RFID tags and readers, particularly in the UHF region, is subject of current research topics. This paper presents a simulation-based approach, using spread-spectrum techniques to reckon the range between UHF RFID tags and a reader system. The UHF-RFID reader reads out the surrounding tags within its reading range, with each tag containing information about its own location. Accordingly, the reader reads the location of each tag, hence being able to generate a basic map. To define the most likely position of the reader itself, it must estimate the distance to each of the RFID tags. This estimation is provided through a spread-spectrum approach utilizing the complete UHF bandwidth of approximately 150 MHz to achieve a high positioning resolution. This work proposes particular distance estimation techniques and presents results for such distance measurements.**

***Keywords*-Radiofrequency identification, Spread spectrum, Wideband, Communication channels.**

I. INTRODUCTION

The increase in sales of navigation systems [1] follows the trend to know exactly where objects or persons (mostly the person itself) are located. That is one of the reasons why global navigation satellite systems (GNSS) like GPS have become very popular. However, the usage of GNSS systems is rather limited to outdoor navigation. Multipath effects, high fading and blocking of satellite navigation signals usually limit the usage of satellite navigation systems in indoor areas.

In the past, indeed, great efforts were made to handle these drawbacks for the indoor area. WLAN-based systems, for instance, use the received signal strength (RSS) to determine the position of a WLAN device. Unfortunately, these systems need training sequences every now and then, resulting in setting up reference maps with reference points (also known as fingerprinting) [2]. However, WLAN-based navigation systems may be combined with inertial navigation systems to receive a much better accuracy. Ultra-wideband systems (UWB), unlike WLAN systems, calculate the *Time of Arrival* (TOA), *Time Difference of Arrival* (TDOA) and/or *Angle of Arrival* (AOA) in order to obtain the position. One example using UWB-technology is the Ubisense platform [3]. These UWB-based systems can achieve a high accuracy due to their very high bandwidth [4]. Besides the described indoor navigation systems exist a lot more techniques to determine the position, including Infrared, Bluetooth, GSM, etc. For instance, SpotON [5] and LANDMARC [6] are RFID-based navigation systems. Generally, both of these systems are based on measuring the RSS to get the current position. However, both systems, SpotON and LANDMARC, use active RFID tags resulting in higher costs per tag (manufacturing and service). Another RFID-based navigation system is described in [7] and [8]. This system is based on passive RFID transponders working at 13.56 MHz (RFID-HF) using the ISO14443 standard with the MIFARE extension. The major drawback of using RFID-HF technology is the low communication distance.

The work described in this paper pursues the following approach: The navigation system should depend on UHF-RFID technology to allow a higher distance to the tags. Also, the distance to be determined between reader and tag shall not depend upon fingerprints, reference maps, or any other training sequences, including RSS measurements. Nevertheless, the position of the reader shall be detected by evaluating an TOA approach from reader to tag (of course, several tags), whereas the, location-wise, fixed tags, contain their very own positions.

This paper shows some theoretical statements being proofed in different simulation scenarios, which deal with conditions mentioned above.

The paper is organized as follows. Section I gives a brief introduction, whereas Section II describes the scenario of the proposed work. The following section shows more details how the system itself is designed and which techniques are needed to achieve the position determination. Subsequently, Section IV is offering simulation results regarding various channel characteristics. Results are offered in Section V, followed by a conclusion and a reference to future work in Section VI.

II. SCENARIO

This section highlights the initial scenario the following sections will be build upon. Assuming an arbitrarily given room with usually UHF-based RFID transponders tagged to the wall(s) or other fixed, unmovable objects. Also, there is an RFID reader, equipped with an omni-directional antenna, somewhere in the room. Furthermore, the system is simplified by assuming that all antennas (reader and transponder)

 ISBN:978-1-61208-113-7

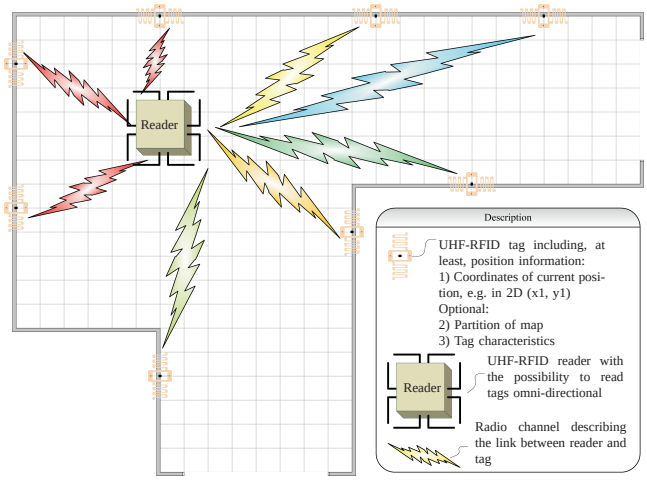

Figure 1. The underlying scenario to deal with

are positioned in the same plane (i.e., 2D, e.g., xy-plane). Figure 1 describes this scenario. The flashes between the reader and the transponders demonstrate the different radio channel links between each reader/transponder pair.

However, the distributed RFID transponders store position data. These position data, at least, consist of latitude, longitude and elevation or just relative coordinates. It is important that every transponder stores its own position; that means reading out a transponder would return its location within the environment. It is assumed that the RFID reader reads out all transponders within the reader's communication range. In that case, the reader knows actually where all the read out tags are located - so that the reader may build a virtual map including the location of every transponder. Unfortunately, the RFID reader itself does not know where it is located. Therefore, the task is to determine the position of the reader within the cloud of transponders, meaning to enable the reader to find its own position by evaluating the radio links to each of the transponders. Assuming additionally, that the reader is able to determine the distance to each transponder, the reader is able to locate itself by evaluating the positions of all transponders.

Of course, there are several ways of estimating the distance between RFID reader and RFID transponder. The previous Section I showed some methods how to estimate the current position using RFID technology, whereas the subsequent Section III describes the proposed approach to determine the distance between an RFID transponder and an RFID reader.

Eexemplary applications of such an RFID-based system for the indoor area would include pedestrian and automatic navigation as well as methods for item searching and position logging.

III. Proposed Work

For estimating the distance between an RFID transponder and the RFID reader, a method very much based on radar techniques [9], particularly pulse compression radar, is suggested. Of course, there are some major differences between a classical pulse compression radar approach and the following proposal.

The reader broadcasts, in addition to the carrier, a broadband signal in the range of the UHF transponders' bandwidth being between 100 MHz and 150 MHz. Due to the high bandwidth, the normalized *signal-to-noise ratio* S/N, also known as E_b/N_0 (energy per bit to noise power spectral density ratio), of the signal is very low. Wide bandwidth signals using low energy are, for instance, ultra-wideband (UWB) signals. UWB signals mainly occur in free-licensed frequency bands, as the signal power is mostly less than the average noise power. In Germany, since 2008, UWB signals below 1.6 GHz may have a spectral power density of -90 dBm/MHz (transmitted power). Assuming room temperature, the noise power per bandwidth is approximately -114 dBm/MHz at the receiver. A path loss of approximately 70 dB (describing the path loss among the way from the reader to the transponder and back) results in an S/N of -46 dB. Using such broad frequency bands and low S/N ratios limit the methods to determine the distance between tag and reader. That is the reason why spread-spectrum (SS) technique is introduced. First, to achieve a processing gain, and second, that due to the higher bandwidth a more accurate positioning resolution is more likely to achieve. The following subsections give some insights into the underlying techniques.

A. Signal Spreading

A technique for coping within such low-S/N environments is called spread-spectrum. Methods of this technique spread signals in order to achieve a higher bandwidth. This technique leads to less interference, jamming, undeliberate detection and some more features [10]. Of course, the transmitter's, but mainly the receiver's architecture gets more complex. Spread-spectrum technique is nowadays fairly common (e.g., WLAN, UMTS, etc.). The spreading method of choice in this work is direct-sequence spread spectrum (DSSS). This method takes the incoming (data) signal and multiplies it with a given spreading sequence. The sequence usually exists of several chips, which have a smaller time period than the bit rate. This leads to a spreaded signal comprising a higher bandwidth but with less signal power per Hertz. Therefore, the power of the signal is spreaded within the frequency domain. Despreading this spreaded signal at the receiver is realized by multiplying the incoming signal with the exact same spreading sequence the transmitter used. Doing so, transforms the former spreaded signal into a narrowband signal, again. This narrowband signal equals the

 ISBN:978-1-61208-113-7

unspreaded data signal in the transmitter, usually with some additive noise aspects in phase, frequency and amplitude.

1) Barker Codes: The performance of the distance determination depends very much on the implemented spreading sequences. There are a lot of sequences, which usually differ in autocorrelation performance, peak side-lobes, orthogonality, etc. As orthogonality is not of interest as there is no multi-user system (as e.g., described in [11]), only the performance of the autocorrelation and the distance to the highest peak side-lobes do matter. A good and simple choice of adequate codes are Barker codes [12]. Usually, Barker codes are used in radar and synchronization applications. The 13-Bit Barker code is the only one with a side-lobe of maximum $+1$. Another bunch of codes, called the PN-codes (pseudo noise codes), can be used, too. These codes may be created using shift registers. They have a slightly smaller performance compared to Barker codes, but with the advantage of being as long as wanted and, of course, flexible in means of being soft-coded (i.e. implemented in software). In order to keep it simple, the 13-Bit Barker code is used so far.

2) Cross-Correlation of Spreaded Signals: The question is how to get positioning data out of these spreaded data signals. As the transmitted signal is known *a priori*, and the reflected, received signal from the tag is known at the reader, too, both signals can be correlated to get the desired TOA measurement. Assuming a simple additive white Gaussian noise channel (AWGN), in which the received signal is only time-shifted compared to the transmitted signal (with more or less noise power); processing a cross-correlation between the transmitted signal (time delay = 0) and the received signal (time delay > 0), a correlation peak arises at the delayed moment of time. If the transmitted signal is shifted in time, that this correlation peak is at $\tau = 0$, then the time difference between transmitted and received signal may be evaluated, as well as the distance to the RFID tag. An example is given in Figures 2 and 3, in which the transmitted and the noisy received baseband signals (Figure 2, shifted by $t = 20$) are cross-correlated (Figure 3). The peak of the correlation function is found at $\tau = 19.88$. Due to the additional noise the peak of the signal is not directly at $\tau = 20$, as the peak detection is processed by using quadratic approximation.

B. Coherent Addition

In the example above, the S/N of the received signal is still 3 dB, leading to an appropriate cross-correlation. Unfortunately, the S/N ratio within a real system would be in the range of -50 dB and even less at the receiver. Therefore, the peak detection would fail very often respectively not delivering a proper result.

Improving the S/N of a signal could be achieved through the usage of coherent addition. This means, that the incoming signals are added to each other in such a manner, that the timing issues from on signal frame to another stays constant (coherent). In other words, the noise, which is assumed to be Gaussian distributed, is canceled out. According to the Cramer-Rao lower bound [13], the S/N ratio is linear proportional to the number of coherent additions, under the assumption that the error variance does not depend upon both parameters. This is proved in simulations and further discussed in Section IV.

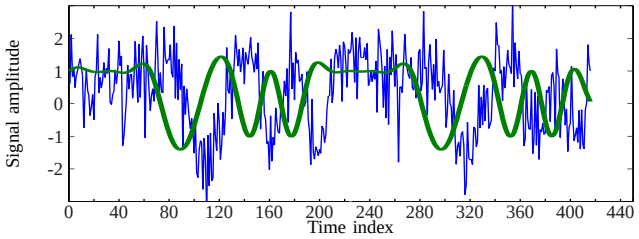

Figure 2. Transmitted (thick) and received (thin) baseband signal at the RFID reader (Inphase component)

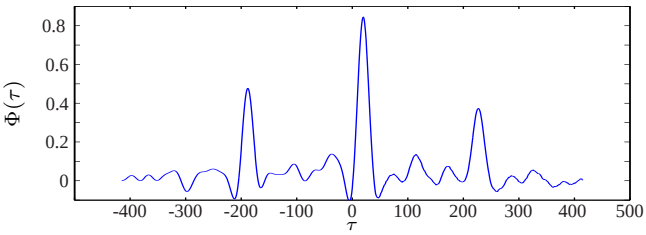

Figure 3. Cross-correlation $\Phi(\tau)$ between transmitted and received baseband signal (Figure 2) at the reader

To highlight the effect of coherent addition, Figure 4 shows the signal differences for an S/N of -20 dB with resulting signals taken at $n = 1$, 10, 100, 1,000 and 10,000 coherent additions. Easy to recognize, that the S/N is increasing with the number of additions.

The objective is to find an accurate (i.e., minimal) number of coherent additions n, to finally have a low error variance σ^2 for the peak detection, as this is a direct indicator for the distance measurement, because the peaks itself determine the distances between reader and tags.

C. Radio channels

As an example of the radio channels used in this work, two different frequency-selective fading channels (presence of multipath) are assumed. Both channels have an excess delay of $127 \times 100\,\text{ps} = 12.7\,\text{ns}$. The channels are build upon 128 discrete impulses, each with a distance of 100 ps to each other. The first pulse (at $\tau = 0$) is a Rician channel with Rician factor $K = 2$, whereas all the other channel impulses are Rayleigh distributed. The average path gain of each channel impulse is formed out of an exponential power delay profile $A_c[\tau]$ as in Equation (1).

$$A_c[\tau] = \frac{1}{T_0} \cdot e^{-\frac{\tau}{T_0}} \;,\; \tau = n \cdot 100\,\text{ps} \;\forall\; n \in [0;127] \cap \mathbb{N}_0 \quad (1)$$

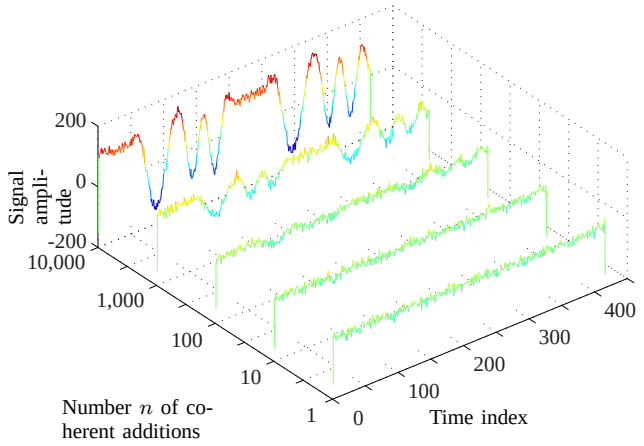

Figure 4. Coherent additions, increasing the S/N ratio

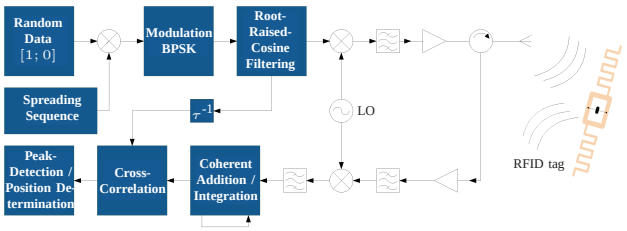

Figure 5. Reader architecture

By changing the value of T_0, different channel characteristics may be formed. A high value of T_0 compared to the symbol period T_s of the signal to be transmitted over the radio channel leads to a highly frequency-selective behavior, whereas a low value of T_0 will lead to a more *flat* channel characteristic. To underline this statement two different values are allocated to T_0 to describe two different radio channels. Channel 1 is characterized with $T_{0,1} = 100 \cdot T_s$, Channel 2 with $T_{0,2} = 0.01 \cdot T_s$. Figure 6 shows the *average* impulse responses of both channels. *Average* means, that the average impulse response consists of the mean of 10.000 simulated channel characteristics as every sub channel impulse is either Rician (at $\tau = 0$) or Rayleigh (at $\tau \neq 0$) distributed. The frequency characteristic of both channels is shown in Figure 7b and 7d together with a one

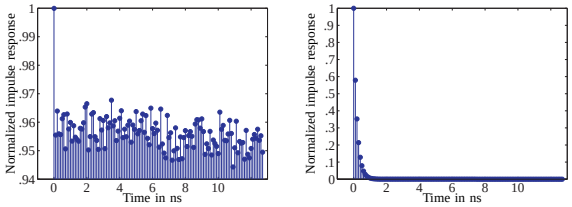

(a) Channel 1 with $T_{0,1} = 100 \cdot T_s$ (b) Channel 2 with $T_{0,2} = 0.01 \cdot T_s$

Figure 6. Average impulse responses of Channel 1 and Channel 2

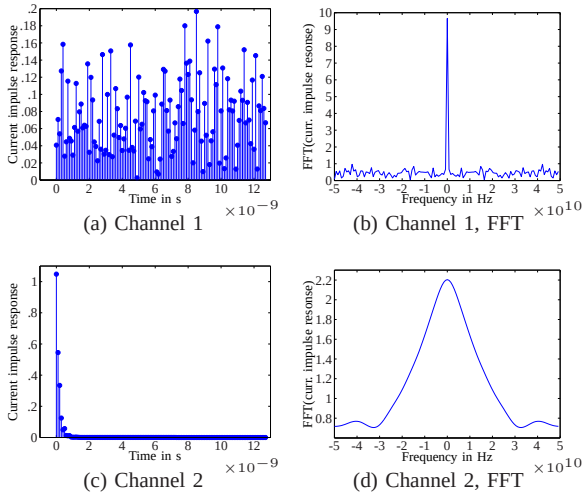

(a) Channel 1 (b) Channel 1, FFT

(c) Channel 2 (d) Channel 2, FFT

Figure 7. Current impulse responses (time and frequency) of Channel 1 and Channel 2

channel time domain representation. As expected, Channel 1 shows a lower coherence bandwidth than Channel 2.

IV. Simulation of Various Scenarios

This section deals with simulations carried out, to evaluate the system's performance and limitations for given radio channels. The first subsection will present simulations for AWGN channels, whereas the following subsections will refer to more realistic radio channels, including real flat fading channels (no multipaths) and frequency-selective radio channels (number of multipaths > 0). All simulations were carried out using a symbol period of $T_s = 10\,\text{ns}$ by using BPSK (binary phase shift keying) and an RRC (root raised cosine)-filter with a roll-off factor of $\beta = 0.5$. This leads to an occupied bandwidth of about 150 MHz. Furthermore, all simulations use the 13-Bit Barker code, which was applied to spread 10 bits of data. The simulations are based on the model as given in Figure 5.

The simulation results show the error variance of the detected peaks σ_p^2 over the number of coherent additions n, whereas the variance refers to the variation of the peaks around its mean value. The upper theoretical limit $\sigma^2_{p,\text{theor.}}$ for the error variance, also referred to as $S/N = \text{-}\infty\,\text{dB}$, is calculated as in Equation (2). The search room for the peaks is arbitrarily limited to about $\pm$ one chip (exact: $1\frac{1}{16}$) with a sample rate of 16 bit per chip. This leads to the limitation of ± 17 in Equation (2).

$$\begin{aligned} \sigma^2_{p,\text{theor.}} &= 1/12\,(\text{Limit}_{\text{upper}} - \text{Limit}_{\text{lower}})^2 \\ &= 1/12\,(2 \cdot 17)^2 = 96.\bar{3} \end{aligned} \quad (2)$$

The theoretical limit is calculated by assuming a continuous uniform distribution of the peaks within the search room and matches an S/N of $\text{-}\infty\,\text{dB}$. The number of channel simulation repetitions in order to receive a significant variance for a given n was set to 100.

 ISBN:978-1-61208-113-7

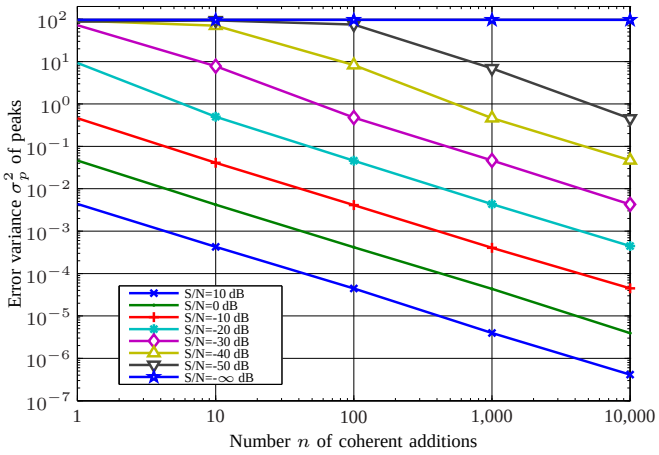

Figure 8. Simulation results for AWGN channel

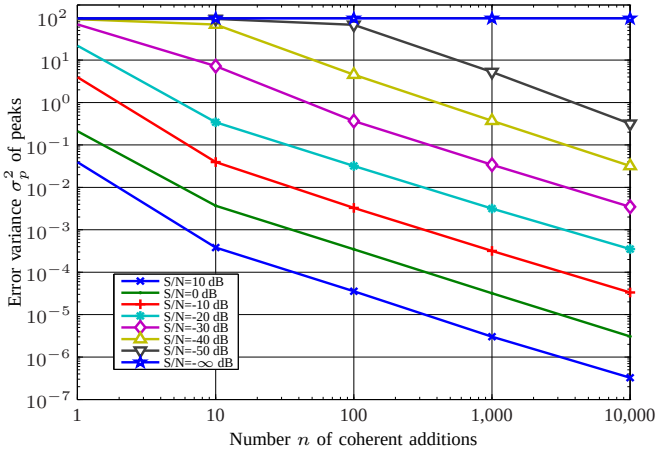

Figure 9. Simulation results for flat fading channel

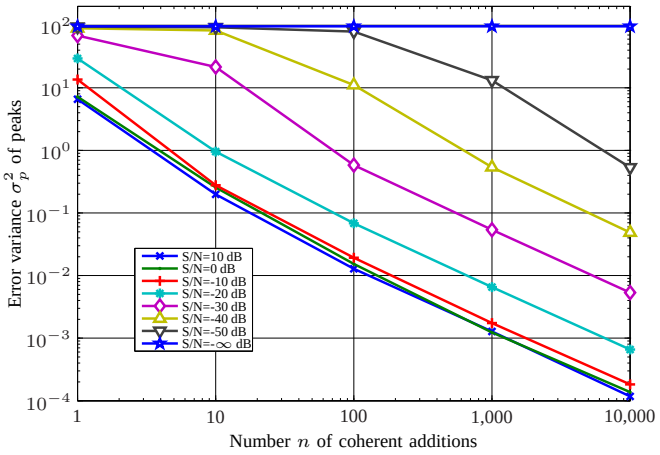

Figure 10. Simulation results for frequency-selective fading channel with $T_0 = 100\,\text{ps}$

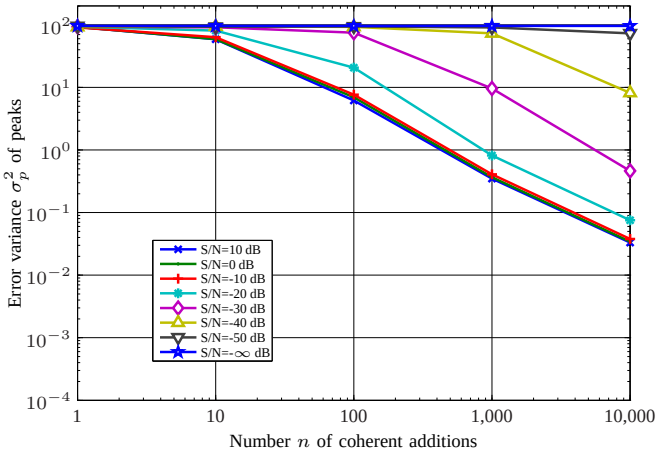

Figure 11. Simulation results for frequency-selective fading channel with $T_0 = 1\,\mu\text{s}$

A. Simulation for AWGN Channel

For a given S/N respectively E_b/N_0 the variance of the error is described over the number of coherent additions n. Refer to Section III for the details of the process.

Figure 8 shows the error variance σ_p^2 over the number of coherent additions n.

B. Simulation for Flat Fading Channel

This subsection shows the simulation results of a flat fading channel, i.e. a Rician distributed radio channel characteristic with no multipaths. Figure 9 shows the simulation results. The K-factor of the Rician channel was $K = 2$.

C. Simulation for Frequency-Selective Fading Channels

This subsection shows the simulation results of two frequency-selective fading channels, inheriting a Rician distributed radio channel characteristic with 127 Rayleigh distributed multipaths. The first simulation (Figure 10) refers to the frequency-selective fading Channel 2 (Figure 6b) with an $T_{0,2} = 0.01 \cdot T_s = 100\,\text{ps}$. As the signal symbol period $T_s = 10\,\text{ns}$ is greater (by a factor of 100) compared to $T_{0,2}$, this channel can be described as rather flat. On the other hand, the frequency-selective fading Channel 1 (Figure 6a) with an $T_{0,1} = 100 \cdot T_s = 1\,\mu\text{s}$ is really frequency-selective as the symbol period is much smaller (factor 100) than $T_{0,1}$. The simulation results of Channel 1 are shown in Figure 11.

V. Results

The simulations carried out in Section IV show three aspects. One is the fact, that the theoretical assumption of the error variance σ_p^2 being linear dependent on the reciprocal of the S/N and the number of coherent additions n could be proofed through simulation. This conclusion is valid for the AWGN channel and for the flat fading channel, at least if the values of the error variance are not close to

 ISBN:978-1-61208-113-7

the theoretical limit. The same assumption is almost valid for the frequency-selective channel, on condition, that the symbol period is much longer than the overall (average) channel excess time, which, of course, leads to a more flat fading channel characteristic. As expected, the error variance increases for a *real* frequency-selective channel (symbol period is smaller than the overall (average) channel excess time), as seen in Figure 11.

The second aspect is the upper theoretical limit of the error variance, which is valid for all channel simulations; refer to Figures 8, 9, 10 and 11.

The third aspect concerns the lower limit of the simulations regarding the frequency-selective fading channels (Figure 10 and 11). An improvement of the S/N to values greater than -10 dB would not lead directly to a smaller error variance in contrast to the AWGN channel (Figure 8) and the flat fading channel (Figure 9). This phenomenon may be explained through the influence of the intersymbol interference (ISI) of the described frequency-selective channels.

Furthermore, an important issue to focus on is the choice of an appropriate channel model. This model may be generated by either measuring out indoor areas (site-specific approach) or defining a statistical model (site-general approach). Both approaches show advantages, but for an ubiquitous estimation, at least for indoor environments, the site-general approach is more useful (see Equation (1)). This may easily understood by assuming that indoor environments change very fast (doors opening and closing, people, interior positions change, etc.). Anyway, a statistical model should be close to a worst-case scenario to provide a lower bound for the error variance of the distance.

Last carried out simulations show, that with a given maximum standard deviation σ_x of 15 cm, a sample rate of $f_s = 1.6$ GHz, and an occupied bandwidth of 150 MHz, the minimum number of coherent additions, to achieve that standard deviation, is 1877 . This result is valid for an AWGN channel model with an average S/N of -40 dB. Finally, the total measurement time is approximately 2.44 ms.

VI. Conclusion & Future Work

The paper presents an approach to estimate the position of an RFID reader by detecting the distance to the surrounding UHF-RFID transponders. As the tags contain their very own location, the reader may generate a basic map with the transponders' locations and its own position by evaluating the distances to the tags with the usage of various techniques. These techniques include spread-spectrum, coherent addition and cross-correlation approaches. The reader exploits the maximum bandwidth the UHF-tags provide (approximately 150 MHz) to achieve a high positioning resolution. In order to estimate the error variance σ_p^2 of the distance to the tags, various simulations were carried out considering varying channel characteristics to get a more realistic valuation of indoor attributes.

Future work would include, more channel characteristics as well as the non-linear behavior of the underlying UHF-RFID tags.

References

[1] RNCOS E-Services Private Limited, "World GPS Market Forecast to 2013," *Research and Markets*, Apr 2009. [Online]. Available: http://www.researchandmarkets.com/reportinfo.asp?report_id=836704

[2] P. Bahl and V. Padmanabhan, "RADAR: An in-building rf-based user location and tracking system," in *IEEE infocom*, vol. 2. Citeseer, 2000, pp. 775–784.

[3] P. Steggles and S. Gschwind, "The Ubisense smart space platform," in *Adjunct Proceedings of the Third International Conference on Pervasive Computing*, vol. 191, 2005.

[4] B. Waldmann, R. Weigel, and P. Gulden, "Method for high precision local positioning radar using an ultra wideband technique," in *Microwave Symposium Digest, 2008 IEEE MTT-S International*, June 2008, pp. 117–120.

[5] J. Hightower, R. Want, and G. Borriello, "SpotON: An indoor 3D location sensing technology based on RF signal strength," *UW CSE 00-02-02, University of Washington, Department of Computer Science and Engineering, Seattle, WA*, 2000.

[6] L. Ni, Y. Liu, Y. Lau, and A. Patil, "LANDMARC: indoor location sensing using active RFID," *Wireless Networks*, vol. 10, no. 6, pp. 701–710, 2004.

[7] A. Loeffler, U. Wissendheit, H. Gerhaeuser, and D. Kuznetsova, "GIDS - A system for combining RFID-based site information and web-based data for virtually displaying the location on handheld devices," in *RFID, 2008 IEEE International Conference on*, April 2008, pp. 312–319.

[8] A. Loeffler, U. Wissendheit, and D. Kuznetsova, "Using RFID-Capable Cell Phones for Creating an Extended Navigation Assistance," in *IMOC 2009*, nov 2009.

[9] J. Taylor, *Ultra-wideband radar technology*. CRC Press, 2001.

[10] M. Simon, J. Omura, R. Scholtz, and B. Levitt, *Spread spectrum communications handbook*. McGraw-Hill New York, 1994.

[11] A. Loeffler, F. Schuh, and H. Gerhaeuser, "Realization of a CDMA-Based RFID System Using a Semi-Active UHF Transponder," in *Wireless and Mobile Communications, 2010. ICWMC 2010. Sixth International Conference on*, September 2010, pp. 5–10.

[12] R. Barker, "Group synchronizing of binary digital systems," *Communication theory*, pp. 273–287, 1953.

[13] G. MacGougan, K. O'Keefe, and R. Klukas, "Ultra-wideband ranging precision and accuracy," *Measurement Science and Technology*, vol. 20, no. 9, p. 5105, 2009.

 ISBN:978-1-61208-113-7